

2
3 **Heat Transfer of Mixed Convection Electroconductivity Flow of Copper**
4 **Nanofluid with Different Shapes in a Porous Micro Channel Provoked**
5 **by Radiation and First Order Chemical Reaction**
6

7
8 **Abstract:**

9 This work presents a theoretical description of different shapes of copper
10 nanoparticle in water based fluid. Analytical solution of the governing
11 hydrodynamic equations and graphs plotted using Mathematica 9.0 software,
12 showed that heat transfer is rapid due to the presence of radiation. Increase
13 in radiation and chemical reaction also led to a corresponding increase in the
14 temperature and concentration profiles of the nanofluid respectively. For the
15 velocity profile of the nanofluid, nanoparticles volume fraction is the only
16 parameter that its increase, increases the velocity profile of the copper
17 nanofluid but Reynolds number, Grashof's number and electroconductivity,
18 result to decrease in the velocity profile of the copper nanofluid. The effect
19 of Nusselt number, Sherwood number and skin friction on the nanofluid is
20 also determined.

21
22 **Key Words- : Heat transfer, Copper, Nanofluid, Porous Channel, Water Based**
23 **Fluid**

24
25 **Notation**

26 ρ_{nf} density of nanofluid
27 P pressure of fluid
28 u dimensionless fluid velocity
29 μ_{nf} dynamic viscosity of nanofluid
30 $(\rho\beta)_{nf}$ thermal expansion coefficient of nanofluids due to temperature
31 σ_{∞} constant fluid electronconductivity
32 U plate velocity
33 k_0 porosity of the medium
34 k_{nf} thermal conductivity of nanofluid
35 q radiative heat flux
36 g acceleration due to gravity
37 k_f thermal conductivity of base fluid
38 ϕ nanoparticles volume fraction
39 ρ_f density of base fluid

40	ρ_s	density of nanoparticles
41	$(\rho C_p)_{nf}$	heat capacitance of nanofluids
42	β_s	volumetric coefficient of nanoparticles
43	β_f	volumetric coefficient of base fluid
44	$(C_p)_f$	specific heat capacity of base fluid
45	$(C_p)_s$	specific heat capacity of nanoparticles
46	C'	concentration of fluid
47	C	dimensionless concentration of fluid
48	T	temperature of fluid
49	θ	dimensionless temperature of fluid
50	Re	Reynolds number
51	Pe	Peclet number
52	Gr_T	thermal Grashof number
53	Gr_C	concentration Grashof number
54	N	dimensionless radiation term
55	k_∞	dimensionless chemical reaction term
56	k_r^2	chemical reaction term
57	λ_n	thermal conductivity ratio
58	D_{nf}	molecular diffusivity
59	u'	fluid velocity

61 1. Introduction

62 Thermal conductivity of heat transfer in fluids is key in the development of energy
63 efficient heat transfer equipment. Conventional heat transfer fluids such as water,
64 oil, ethylene glycol mixtures to mention few, are poor heat transfer fluids. With
65 global need for improvement, to develop advanced heat transfer fluids with
66 significantly higher thermal conductivities than those presently available is of
67 utmost necessity. Touloukian et al (1970) has opined that at room temperature,
68 **metals in solid form have orders of magnitude higher that those of solids. The**
69 new class of heat transfer fluids that are engineered by suspending nanometer-
70 sized particles in conventional heat transfer fluids whose averaged sized particles
71 is below 50nm is termed nanofluids Choi (1995) The reality is that in today's
72 science and technology, size does matter, therefore modern fabrication technology
73 provides great opportunity to actively process materials at the micro and
74 nanometer scales. The impact of this new heat transfer technology is important
75 due to its performance in thermal conductivity and viscosity which led to
76 improved heat transfer and stability, reduced pumping power, minimal clogging
77 and miniaturized systems as well as cost and energy savings (Choi et al 1992a and
78 1992b). The different composition of nanoparticles in base fluids to form
79 nanofluids has its application in power generation and electronic equipment just
80 to mention few. The applications of nanofluids is predicated on the desirable
81 properties or qualities following Mukherjee and Paria (2013) as follows (i) rapid

82 increase in thermal conductivity (ii) ultrafast heat transfer ability (iii) reduce
83 pumping power (iv) reduce friction coefficient (v) reduce clogging in
84 microchannels (vi) improved stability than other colloids and (vii) improved
85 lubrication. Feng et al (2006), examined the preparation of gold, silver and
86 platinum nanofluids using aqueous organic phase transfer method. Yu et al (2010)
87 Wei et al (2010) and Zhu et al (2007), prepared Copper oxide nanofluid and use
88 ammonium citrate to prevent the growth and aggregation of nanoparticles, resulting
89 in a stable CuO aqueous nanofluid with higher thermal conductivity. Other works
90 such as (Hwang, et al (2007) and Li et al(2007), used spectral analysis method to
91 detect stability of nanofluids. Experimental and theoretical studies are abundant
92 on conductivity, viscosity and stability of nanofluids and its aggregate
93 nanoparticles. Duncan and Rouvray (1989), Gliter(1989) and Hashin and
94 Shtrikman (1962) examined nanofluid materials and made far reaching deductions
95 from their findings. The model proposed by Hamilton and Crosser (1962) to
96 predict the thermal conductivity of nanofluid, containing large agglomerated
97 particles and that obtained from experimental results were compared and it fits
98 well, but divergence is observed at low volume fractions. The implication of this
99 observation is that particle size and shape dominate thermal conductivity of
100 nanofluids (Li 1998). Studies on nanoparticles of spherical shapes are many but
101 limited in applications and significance, Aaiza et al (2105). As a result of this
102 assertion, a non spherical shaped nanoparticle is chosen for this study in four
103 different shapes, namely, platelet, cylinder, blade and brick. The choice of non
104 spherical shape nanoparticle is predicated on the work of Aaiza et al (2015),
105 where they mentioned desirable properties in cancer treatment. Asma et al (2015),
106 studied free convection flow of nanoparticles including ramped wall temperature
107 using five different types of spherical shape nanoparticles and reported that the
108 solution of the governing equations was exact. Heat transfer due to mixed
109 convection is experienced in many physical situations and occur as the flow in a
110 channel due to the process of heating or cooling of the channel walls. This
111 experience is a combination of free convection and forced convection. Some
112 researches have been reported, they include (Sebdani et al (2012), Sheikhzabeh et
113 al (2012), Nadeem and Saleem (2014) and Al-Salem et al(2012) in which mixed
114 convection and nanofluid were discussed in different nanoparticles shape and
115 configurations. Aaiza et al (2105), investigated water based nanofluid and
116 ethylene glycol based nanofluid and reported that viscosity and thermal
117 conductivity are the most prominent parameters responsible for different results of
118 velocity and temperature. The present study is to examine the effect of first order
119 chemical reaction and electroconductivity on radiative heat transfer in mixed
120 convection flow in a micro porous channel with different shapes of copper (Cu) in
121 water based nanofluid. The Cu in water based nanofluid preparation and
122 sphericity is reported in Yimin and Li (2000). The reason is that Cu as a
123 nanoparticle, possesses higher thermal conductivity and stability than other
124 nanofluids. The focus is to consider non spherical shaped nanofluid under the no
125 slip boundary conditions with bounding walls of the channel at rest, the upper
126 wall in motion and lower at rest and both walls are in motion. Solutions to
127 velocity, temperature and concentration profile with graphical results and

128 parameters of interest discussed, which is an extension of the work of Aaiza et al
 129 (2105)

130

131

132 2. Formulation of the problem

133 The assumption of the effect of induced magnetic field is small, therefore, neglected.

134 Also the usual Boussinesq approximation is assumed. The no slip condition at the

135 boundary wall is considered. The x-axis is taken along the flow and y-axis is taken

136 normal to the flow direction. The governing hydrodynamic equations are given as

$$137 \rho_{nf} \frac{\partial u'}{\partial t'} = -\frac{\partial p}{\partial x'} + \mu_{nf} \frac{\partial^2 u'}{\partial y'^2} - u' \left(\frac{\sigma_{\infty}}{U} + \frac{\mu_{nf}}{k_0} \right) + (\rho\beta_T)_{nf} g(T - T_0) + (\rho\beta_c)_{nf} g(C - C_0) \quad (1)$$

138

$$139 (\rho C_p)_{nf} \frac{\partial T}{\partial t'} = k_{nf} \frac{\partial^2 T}{\partial y'^2} - \frac{\partial q}{\partial y} \quad (2)$$

140

$$141 (\rho C_p)_{nf} \frac{\partial C'}{\partial t'} = D_{nf} \frac{\partial^2 C'}{\partial y'^2} - k_r^2 C' \quad (3)$$

142 With the boundary conditions

$$143 u'(0, t) = 0, \quad u'(d, t) = 0, \quad (4)$$

144

$$145 T(0, t) = T_0, \quad T(d, t) = T_w \quad (5)$$

146

$$147 C'(0, t) = C_0, \quad C'(d, t) = C_w \quad (6)$$

148 where following Boricic et al. (2005), the fluid electroconductivity is assumed to be of

149 the form $\sigma_{\infty} \left(1 - \frac{u'}{U} \right)$ but for physical exigency and mathematical amenability, it is

150 approximated to the form in equation (1) Ngiangia and Harry (2017).

151

152 According to a model proposed by Hamilton and Crosser (1962), the thermal

153 conductivity and dynamic viscosity is assumed valid for both spherical and non spherical

154 shapes nanoparticles. The model is stated as

155

$$156 \mu_{nf} = \mu_f (1 + a\phi + b\phi^2) \quad (7)$$

157

$$158 \frac{k_{nf}}{k_f} = \frac{k_s + (n-1)k_f + (n-1)(k_s - k_f)\phi}{k_s + (n-1)k_f - (k_s - k_f)\phi} \quad (8)$$

159 where $n = \frac{3}{\psi}$ is the empirical shape factor and ψ is the sphericity, a ratio of surface area

160 of sphere to surface area of real particle with equal volumes as in **table 1** with **a** and **b** as

161 constant empirical shape factors.

162

163 Another expression by Wasp(1977) to determine the effective thermal conductivity of
 164 solid-liquid mixture is given as

$$165 \frac{k_{eff}}{k_f} = \frac{k_s + 2k_f - 2\phi(k_f - k_s)}{k_s + 2k_f - \phi(k_f - k_s)} \quad (9)$$

167 This is a special case of equation (8) with sphericity 1.0

168

169

170 From equations (1), (2) and (3), ρ_{nf} , $(\rho\beta)_{nf}$ and $(\rho C_p)_{nf}$ following Asma et al (2015) is
 171 derived as

$$172 \begin{aligned} \rho_{nf} &= (1-\phi)\rho_f + \phi\rho_s \\ (\rho\beta)_{nf} &= (1-\phi)(\rho\beta)_f + \phi(\rho\beta)_s \\ (\rho C_p)_{nf} &= (1-\phi)(\rho C_p)_f + \phi(\rho C_p)_s \end{aligned} \quad (10)$$

173 In the work of Makinde and Mhone (2005), the plates temperature T_0 and T_w are usually
 174 high and produces radiative heat transfer. According to Cogley et al (1968), for optically
 175 thin medium with relatively low density, the radiative heat flux is given by

176

$$177 \frac{\partial q}{\partial y} = 4\delta^2(T - T_0) \quad (11)$$

178 where δ is the radiation absorption coefficient

179 Substituting equation (11) into equation (2) and using the following dimensionless
 180 variables

$$181 \begin{aligned} x &= \frac{x'}{d}, y = \frac{y'}{d}, u = \frac{u'}{U}, t = \frac{t'U}{d}, \frac{\partial p}{\partial x'} = \lambda \exp(i\omega t), \theta = \frac{T - T_0}{T_w - T_0}, \text{Re} = \frac{Ud}{\mu_f} \\ k &= \frac{k_0}{d^2}, Gr_T = \frac{g\beta_f d^2 (T_w - T_0)}{\mu_f U}, Gc_T = \frac{g\beta_c d^2 (C' - C_0)}{\mu_f U}, \sigma_0 = \frac{\sigma_\infty \mu_f dt}{U} \\ N &= \frac{4\delta^2 d^2}{k_f}, Pe_T = \frac{Ud(\rho C_p)_f}{k_f}, Pe_c = \frac{Ud(\rho C_p)_f}{D_{nf}}, k_\infty = \frac{k_r T_0}{\sigma_\infty U^2}, \lambda_n = \frac{k_{nf}}{k_f} \end{aligned}$$

182 Further, we define

183

$$184 w_1 = (1-\phi) + \phi \frac{\rho_s}{\rho_f} \quad w_2 = (1 + a\phi + b\phi^2) \quad w_3 = (1-\phi)\rho_f + \phi \frac{(\rho\beta)_s}{\beta_f}$$

$$185 w_4 = \left[(1-\phi) + \phi \frac{(\rho C_p)_s}{(\rho C_p)_f} \right] \quad a_1 = w_1 \text{Re} \quad a_2 = \sigma_0 + \frac{w_2}{k} \quad a_3 = w_3 Gr_T$$

$$186 a_4 = w_3 Gr_c, c_1 = \frac{Pe_c w_4}{\lambda_n} \quad b_1 = \frac{Pe_T w_4}{\lambda_n} \quad b_2 = \frac{N}{\lambda_n}, c_2 = \frac{k_\infty}{\lambda_n},$$

187 then equations (1), (2) and (3) takes the form

$$188 \quad a_1 \frac{\partial u}{\partial t} = \lambda \varepsilon \exp(i\omega t) + w_2 \frac{\partial^2 u}{\partial y^2} - a_2 u + a_3 \theta + a_4 C \quad (12)$$

$$189 \quad b_1 \frac{\partial \theta}{\partial t} = \frac{\partial^2 \theta}{\partial y^2} - b_2 \theta \quad (13)$$

$$190 \quad c_1 \frac{\partial C}{\partial t} = \frac{\partial^2 C}{\partial y^2} - c_2 C \quad (14)$$

191 Subject to the boundary conditions

$$192 \quad u(0, t) = 0, \quad u(1, t) = 1 \quad t > 0 \quad (15)$$

$$193 \quad \theta(0, t) = 0, \quad \theta(1, t) = 1 \quad t > 0 \quad (16)$$

$$194 \quad C(0, t) = 0, \quad C(1, t) = 1 \quad t > 0 \quad (17)$$

195

196 3. Method of Solution

197

198 To solve equations (12-14), we assume solution of the form

199

$$200 \quad u(y, t) = [u_0(y) + \varepsilon \exp(i\omega t)u_1(y)] \quad (18)$$

$$201 \quad \theta(y, t) = [\theta_0(y) + \varepsilon \exp(i\omega t)\theta_1(y)] \quad (19)$$

$$202 \quad C(y, t) = [C_0(y) + \varepsilon \exp(i\omega t)C_1(y)] \quad (20)$$

203 where ε is a small parameter

204

205 **Case 1:** Both walls of the channel are kept stationary, while the temperature of the upper
206 wall of the channel is assumed constant, the lower wall has uniform temperature and the
207 boundary conditions conform to equations (18-20).

208 We substitute equation (20) into equation (14) and simplify, the result is

209

$$210 \quad C_0''(y) - c_2 C_0(y) = 0 \quad (21)$$

$$211 \quad C_1''(y) - (c_1 i\omega + c_2)C_1(y) = 0 \quad (22)$$

212 Solving equations (21) and (22) and imposing the boundary conditions of equation (17)
213 as well as substituting in equation (20), we get

$$214 \quad C(y, t) = \text{Sinh}\sqrt{c_2} y + \varepsilon \exp(i\omega t)\text{Sinh}\sqrt{\beta} y \quad (23)$$

215 where $\beta = c_1 i\omega + c_2$

216 Similarly, we put equation (19) into equation (13) and the resulting expression takes the
217 form

218

$$219 \quad \theta_0''(y) - b_2 \theta_0(y) = 0 \quad (24)$$

$$220 \quad \theta_1''(y) - (b_1 i\omega + b_2)\theta_1(y) = 0 \quad (25)$$

221 The solutions of equations (24) and (25) and imposition of the boundary conditions of
222 equation (16) as well as put the entire expression into equation (19), gives

223

$$224 \quad \theta(y, t) = \text{Sinh}\sqrt{b_2} y + \varepsilon \exp(i\omega t)\text{Sinh}\sqrt{\beta_2} y \quad (26)$$

225 where $\beta_2 = b_1 i\omega + b_2$

226 Also, following the same procedure and the boundary conditions of equation (18), the
 227 solution of equation (12) is

$$u(y, t) = \beta_5 \text{Sinh} \sqrt{\frac{a_2}{w_2}} y + \beta_3 \text{Sinh} \sqrt{b_2} y + \beta_4 \text{Sinh} \sqrt{c_2} y +$$

$$\varepsilon \exp(i\omega t) \left(-\beta_8 \text{Cosh} \sqrt{\frac{a_1 + a_2}{w_2}} y + \beta_9 \text{Sinh} \sqrt{\frac{a_1 + a_2}{w_2}} y + \beta_6 \text{Sinh} \sqrt{\beta_2} y + \beta_7 \text{Sinh} \sqrt{\beta} y + \beta_8 \right)$$

228
 229 (27)
 230

$$231 \text{ where, } \beta_3 = \frac{-\frac{a_3}{w_2}}{b_2^2 - \frac{a_2}{w_2}}, \quad \beta_4 = \frac{a_4}{w_2(c_2^2 - 1)}, \quad \beta_5 = \frac{-\beta_3 \text{Sinh} \sqrt{b_2} - \beta_4 \text{Sinh} \sqrt{c_2}}{\text{Sinh} \sqrt{\frac{a_2}{w_2}}},$$

$$232 \beta_6 = \frac{-\frac{a_3}{w_2}}{\beta_2 - \frac{a_1 + a_2}{w_2}}, \quad \beta_7 = \frac{-\frac{a_4}{w_2}}{\beta - \frac{a_1 + a_2}{w_2}}, \quad \beta_8 = \frac{\lambda}{a_1 + a_2},$$

$$233 \beta_9 = \frac{-(\beta_8 + \beta_6 \text{Sinh} \sqrt{\beta_2} + \beta_7 \text{Sinh} \sqrt{\beta})}{\text{Sinh} \sqrt{\frac{a_1 + a_2}{w_2}}}$$

234 **Case 2:** The upper wall of the channel is set into oscillatory motion while the lower wall
 235 is held stationary and the resulting boundary conditions are given as

$$236$$

$$237 u(0, t) = 0, \text{ and } u(1, t) = H(t)\varepsilon \exp(i\omega t); \quad t > 0 \quad (28)$$

238 where H(t) is the Heaviside step function

239 Imposing the boundary conditions of equation (28) into the solution of equation (12), we
 240 get

241

$$u(y, t) = \left(\frac{H(t)\varepsilon \exp(i\omega t) - \beta_3 \text{Sinh} \sqrt{b_2} - \beta_4 \text{Sinh} \sqrt{c_2}}{\text{Sinh} \sqrt{\frac{a_2}{w_2}}} \right) \text{Sinh} \sqrt{\frac{a_2}{w_2}} y$$

$$242 + \beta_3 \text{Sinh} \sqrt{b_2} y + \beta_4 \text{Sinh} \sqrt{c_2} y$$

$$+ \varepsilon \exp(i\omega t) \left[\left(\frac{H(t)\varepsilon \exp(i\omega t) - \beta_6 \text{Sinh} \sqrt{\beta_2} - \beta_7 \text{Sinh} \sqrt{\beta} - \beta_8}{\text{Sinh} \sqrt{\frac{a_1 + a_2}{w_2}}} \right) \text{Sinh} \sqrt{\frac{a_1 + a_2}{w_2}} y + \beta_{10} \right]$$

243 (29)

244 where $\beta_{10} = \beta_6 \text{Sinh}\sqrt{\beta_2} y + \beta_7 \text{Sinh}\sqrt{\beta} y + \beta_8$

245

246 **Case 3:** In this situation, the two channel walls are set into oscillatory motion and the
 247 resulting boundary conditions (Aiza et al (2105)) are given as

248

249 $u(0, t) = H(t)\varepsilon \exp(i\omega t)$ and $u(1, t) = H(t)\varepsilon \exp(i\omega t) \quad t > 0$ (30)

250 The solution of equation (12), having used the boundary conditions of equation (30),
 251 following the same procedure used in case 2, we obtain

252

$$\begin{aligned}
 u(y, t) = & H(t)\varepsilon \exp(i\omega t) \text{Cosh}\sqrt{\frac{a_2}{w_2}} y + \\
 & \left(\frac{H(t)\varepsilon \exp(i\omega t) - \beta_3 \text{Sinh}\sqrt{b_2} - \beta_4 \text{Sinh}\sqrt{c_2}}{\text{Sinh}\sqrt{\frac{a_2}{w_2}}} \right) \text{Sinh}\sqrt{\frac{a_2}{w_2}} y \\
 & + \beta_3 \text{Sinh}\sqrt{b_2} y + \beta_4 \text{Sinh}\sqrt{c_2} y \\
 & + H(t)\varepsilon \exp(i\omega t) \text{Cosh}\sqrt{\frac{a_1 + a_2}{w_2}} y + \\
 & \left(\frac{H(t)\varepsilon \exp(i\omega t) - \beta_6 \text{Sinh}\sqrt{\beta_2} - \beta_7 \text{Sinh}\sqrt{\beta} - \beta_8}{\text{Sinh}\sqrt{\frac{a_1 + a_2}{w_2}}} \right) \text{Sinh}\sqrt{\frac{a_1 + a_2}{w_2}} y \\
 & + \beta_6 \text{Sinh}\sqrt{\beta_2} y + \beta_7 \text{Sinh}\sqrt{\beta} y + \beta_8
 \end{aligned} \tag{31}$$

253

254

255 **Nusselt number** (Nu) (the rate of heat transfer coefficient)

256

257 From equation (26), the Nusselt number is given by

258 $Nu = -\left(\frac{\partial\theta}{\partial y}\right)_{y=0} = -\left(\sqrt{b_2} + \varepsilon \exp(i\omega t)\sqrt{\beta_2}\right)$ (32)

259 **Sherwood number** (S_b) (the rate of mass transfer coefficient)

260 $S_b = -\left(\frac{\partial C}{\partial y}\right)_{y=0} = -\left(\sqrt{C_2} + \varepsilon \exp(i\omega t)\sqrt{\beta}\right)$ (33)

261 **Skin frictions** (τ)

262 $\left(\frac{\partial u}{\partial y}\right)_{y=0} = \beta_5 \sqrt{\frac{a_2}{w_2}} + \beta_3 \sqrt{b_2} + \beta_4 \sqrt{c_2} + \varepsilon \exp(i\omega t) \left(\beta_9 \sqrt{\frac{a_1 + a_2}{w_2}} + \beta_6 \sqrt{\beta_2} + \beta_7 \sqrt{\beta} \right)$ (34)

263 **Case 2**

$$\left(\frac{\partial u}{\partial y}\right)_{y=0} = \left[\frac{H(t)\varepsilon \exp(i\omega t) - \beta_3 \text{Sinh}\sqrt{b_2} - \beta_4 \text{Sinh}\sqrt{c_2}}{\text{Sinh}\sqrt{\frac{a_2}{w_2}}} \right] \sqrt{\frac{a_2}{w_2}} + \beta_3 \sqrt{b_2} + \beta_4 \sqrt{c_2} + \varepsilon \exp(i\omega t) \left[\frac{H(t)\varepsilon \exp(i\omega t) - \beta_6 \text{Sinh}\sqrt{\beta_2} - \beta_7 \text{Sinh}\sqrt{\beta} - \beta_8}{\text{Sinh}\sqrt{\frac{a_1 + a_2}{w_2}}} \right] \sqrt{\frac{a_1 + a_2}{w_2}} + \beta_{77} \quad (35)$$

265 where $\beta_{77} = \beta_6 \sqrt{\beta_2} + \beta_7 \text{Sinh}\sqrt{\beta}$

266 **Case 3**

$$\left(\frac{\partial u}{\partial y}\right)_{y=0} = \left[\frac{H(t)\varepsilon \exp(i\omega t) - \beta_3 \text{Sinh}\sqrt{b_2} - \beta_4 \text{Sinh}\sqrt{c_2}}{\text{Sinh}\sqrt{\frac{a_2}{w_2}}} \right] \sqrt{\frac{a_2}{w_2}} + \beta_3 \sqrt{b_2} + \beta_4 \sqrt{c_2} + \left[\frac{H(t)\varepsilon \exp(i\omega t) - \beta_6 \text{Sinh}\sqrt{\beta_2} - \beta_7 \text{Sinh}\sqrt{\beta} - \beta_8}{\text{Sinh}\sqrt{\frac{a_1 + a_2}{w_2}}} \right] \sqrt{\frac{a_1 + a_2}{w_2}} + \beta_6 \sqrt{\beta_2} + \beta_7 \sqrt{\beta} \quad (36)$$

268 **4. Discussion**

269
270

271 As a result of increase in the chemical reaction of the nanoparticles and the base fluid, a
272 corresponding increase in the concentration of the nanofluid is observed as depicted in
273 Figure 1

274 Figure 2, showed the effect of radiation on the temperature of copper nanofluid. As a
275 result of high thermal conductivity of nanofluid, increase in radiation of nanofluid result
276 in a corresponding increase in the temperature profile of the nanofluid. This observation
277 is consistent with the work of Aaiza et al (2015) and Timofeeva et al (2009) and a
278 departure from the effect of radiation on other base fluids.

279

280 Figure 3, showed the convective heat transfer coefficient between the nanofluid and the
281 channel walls to estimate the heat transfer performance of the nanofluid. The graph
282 showed that, the heat transfer is rapid (a curve), may be due to the presence of radiation
283 when compared to the work of Xuan and Li (2000) which is a straight line. The peclt
284 number is a parameter to describe such effect. Equation (32) therefore, is a holistic
285 approach to study the improved heat transfer mechanism of the nanofluid.

286

287 From Figure 4, it is shown that the relationship can be used to determine the convective
288 mass transfer coefficient between the nanofluid and the containing inner wall to estimate
289 the improved mass transfer performance of the nanoparticles.

290 Figure 5, clearly demonstrate that, increase in pecelet number correspond to a decrease in
291 the skin friction of the nanofluid.

292

293 Increase in nanoparticles volume fraction of copper nanofluid result in a corresponding
294 increase in the velocity profile of the nanofluid as shown in Figure 6.

295 Reynolds number describe the transition of fluids from laminar to turbulence, since it is a
296 ratio of inertia force to viscous force, its increase as shown in Figure 7, results in a
297 decrease in the velocity profile of nanofluid and this observation is at variance with the
298 results of increase in Reynolds number of base fluids(Ngiangia and Taylor-Harry 2017).
299 Electroconductivity tends to impede the flow of fluid and same observation was noticed
300 as depicted in Figure 8, where increase in electroconductivity enhances the decrease in
301 the velocity of copper nanofluid.

302

303 The Grashof number due to temperature conducts heat away from the channel plates into
304 the nanofluid, thereby increasing the temperature of the fluid but as a result of rapid heat
305 transfer and thermal conductivity of nanofluid, a decrease in velocity profile of the
306 nanofluid is observed as shown in Figure 9.

307

308 Figure 10, showed the effect of different shapes of copper nanoparticles on the velocity
309 of water based nanofluids. The graph clearly depicts that, the highest velocity is recorded
310 with brick followed by cylinder, platelet and finally blade. The effect on shapes of
311 nanoparticles on velocity is also a dependence on viscosity for various volume fractions.

312

313 The following numerical values are used in the plotting of the graphs

$$\lambda_n = 100, \omega = 0.2, t = 1, \lambda = 1, \varepsilon = 0.003, k = 0.3$$

$$Gr_T, Gr_C = 1, 3, 5, 7$$

$$Pe = 0.35, 0.70, 1.05, 1.40$$

$$\phi = 0.1, 0.2, 0.3, 0.4$$

314

$$Re = 100, 1500, 2000, 2500$$

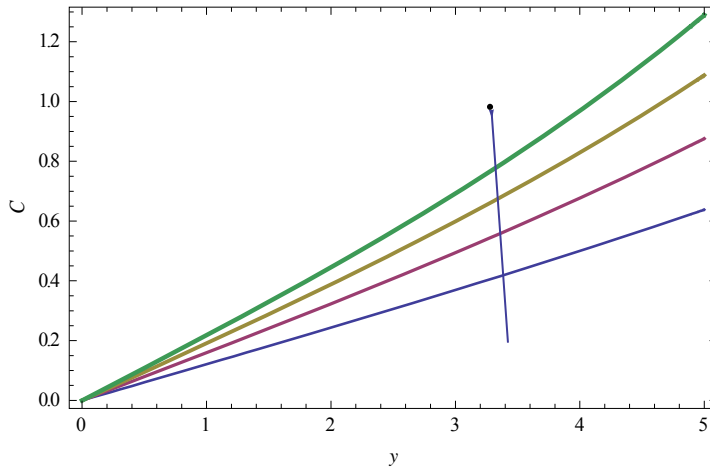
$$N = 2.0, 4.0, 6.0, 8.0$$

$$k_\infty = 1.35, 2.35, 3.35, 4.45$$

$$\sigma_0 = 0.4, 0.8, 1.2, 1.6$$

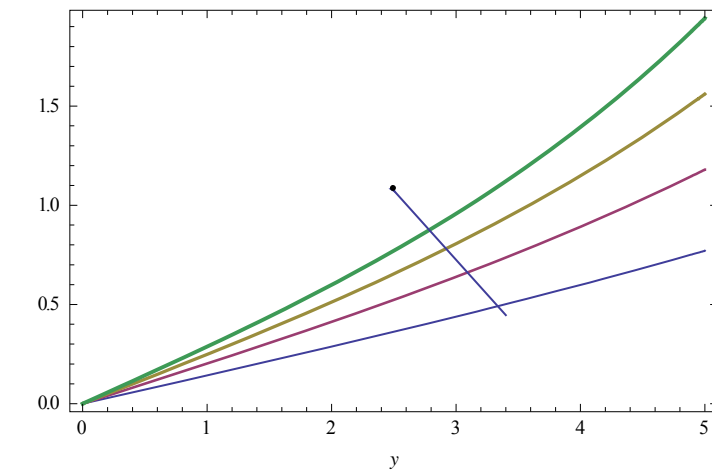
315

316



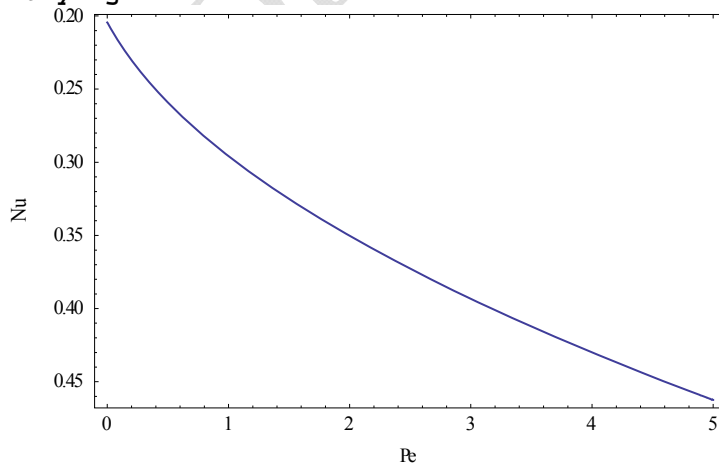
317
318
319
320
321
322

Fig.1. The dependence of concentration on coordinate with chemical reaction k_{∞} varying



323
324
325

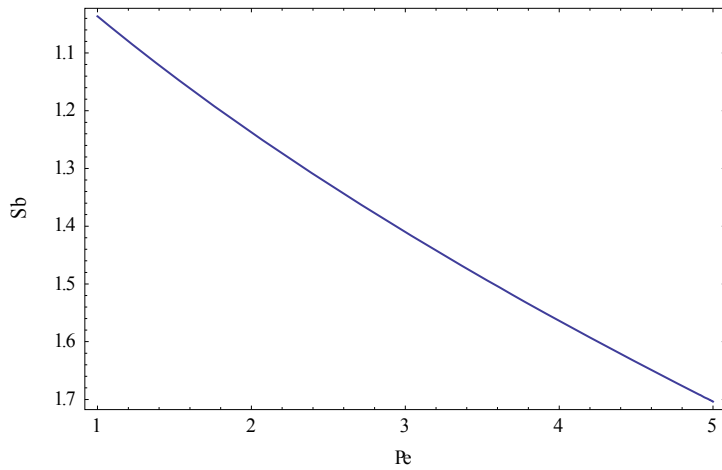
Fig.2. The dependence of temperature on coordinate with radiation N varying



326
327
328

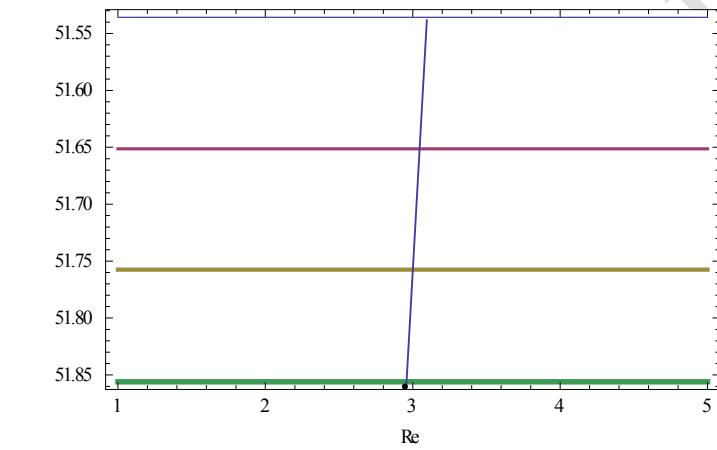
Fig.3. The Nusselt number (Nu) versus Peclet number (Pe)

329
330
331



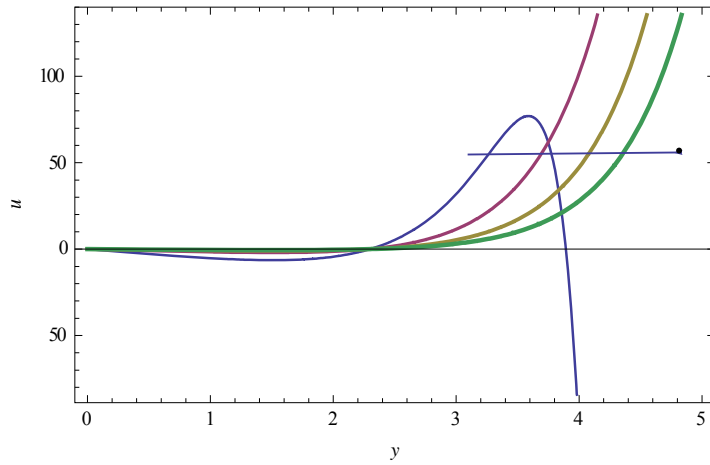
332
333
334
335
336
337

Fig.4. The Sherwood number (Sb) versus Peclet number (Pe)



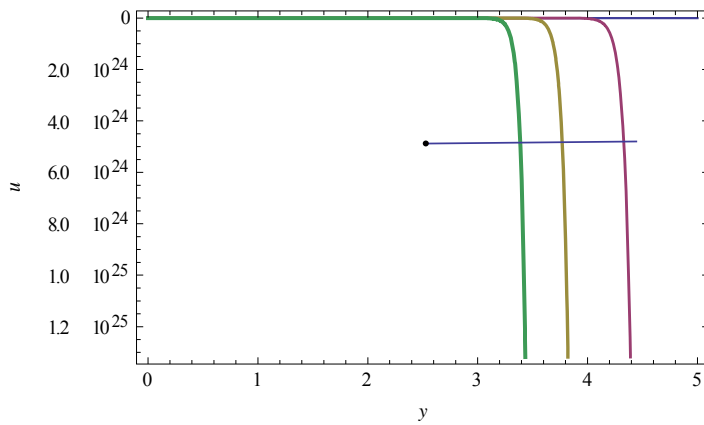
338
339
340
341

Fig.5. The Skin Friction (τ) versus Reynolds number (Re) with Peclet number (Pe) varying.



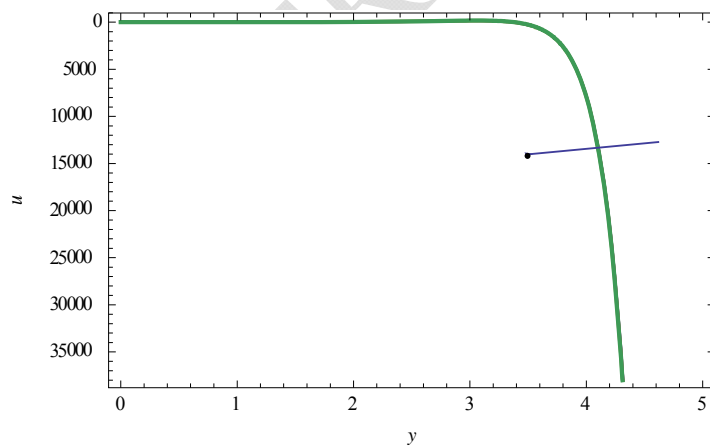
342
343
344
345

Fig.6. The dependence of velocity on coordinate with nanoparticles volume fractions ϕ varying



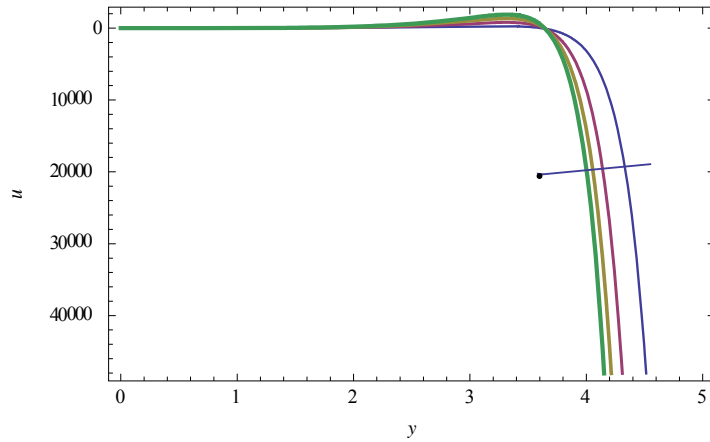
346
347
348
349

Fig.7. The dependence of velocity on coordinate with Reynolds number Re varying

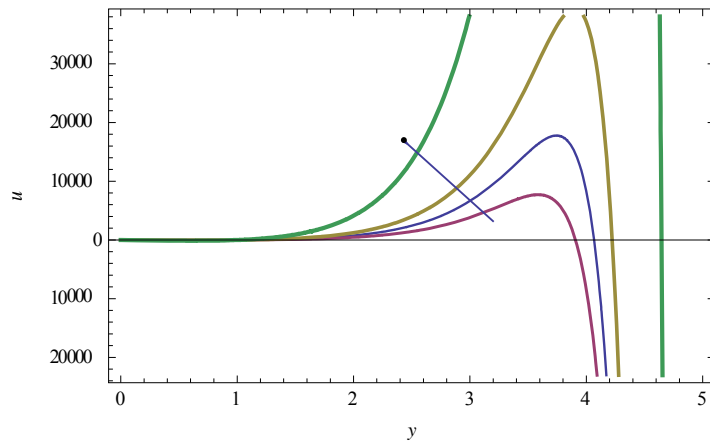


350
351
352
353

Fig.8. The dependence of velocity on coordinate with conductivity σ_0 varying



354
 355 **Fig.9. The dependence of velocity on coordinate with Grashof number Gr_T**
 356 **varying**
 357
 358



359
 360 **Fig.10. The dependence of velocity on coordinate with different nanoshape**
 361 **particles n**
 362

363 **Table 1: Constants a and b empirical shape factors, Timofeeva et al (2009)**

Model	Platelet	Blade	Cylinder	Brick
a	37.1	14.6	13.5	1.9
b	612.6	123.3	904.4	471.4

364
 365 **Table 2: Sphericity for different shapes nanoparticles, Timofeeva et al (2009)**

Model	Platelet	Blade	Cylinder	Brick
ψ	0.52	0.36	0.62	0.81

366
 367 **Table 3; Thermophysical properties of water and nanoparticle, Timofeeva et al (2009)**

Model	$\rho(kgm^{-3})$	$C_p(kg^{-1}K^{-1})$	$k(Wm^{-1}K^{-1})$	$\beta \times 10^{-5} K^{-1}$
Water (H_2O)	997.1	4179	0.613	21
Copper (Cu)	8933	385	401	1.67

368
 369

370 **5. Conclusions**

371 A perturbation technique on the description of the heat and mass transfer of copper
372 nanofluid has been carried out. An essential characteristic of nanofluid, in particular
373 copper nanoparticles in water based fluids is that, as a result of its high thermal
374 conductivity and heat transfer ability, the effect on velocity profile is significantly
375 different from other conventional base fluids. Experiments is needed for industrial,
376 scientific and engineering applications of copper nanaofluid and others. It should be
377 noted that the improved performance of the copper nanofluid is not limited to its high
378 thermal conductivity and heat transfer ability but also from the random movement and
379 dispersion effect on the nanoparticles. The effect of Grashof number on the concentration
380 of nanofluid was ignored because the result is the same as that of the temperature.

381

382 **REFERENCES**

383 Aaiza, G; Khan I and Shafie S. 2015. Energy Transfer in Mixed Convection MHD Flow
384 of Nanofluid Containing Different Shapes of Nanoparticles in a Channel Filled with
385 Saturated Porous Medium. *Nanoscale Research Letters*. 10(490): 1-14.

386 Al-Salem, K, Oztop, H. F, Pop, I and Varo, Y. 2012. Effect of Moving lid Direction on
387 MHD Mixed Convection in a linearly Heated Cavity. *International Journal of Heat and
388 Mass Transfer*. 55, 1103-1112.

389

390 Asma, K, Khan, I and Sharidan, S 2015. Exact Solutions for Free Convection Flow of
391 NanoFluids with Ramped Wall Temperature. *The European Physical Journal Plus*. 130,
392 57-71.

393

394 Boricic, Z, Nikodijevic D, Milenkovic D, and Stamenkovic Z.2005. A form of MHD
395 universal equation of unsteady incompressible fluid flow with variable
396 electroconductivity on heated moving plate *Theoretical and Applied Mechanics*. 32(1),
397 65-77.

398

399 Choi, U. S,. 1995. Enhancing Thermal Conductivity of Fluids with Nanoparticles.
400 *Development and Applications of Non-Newtonian Flows*. Eds. D. A. 99-105.

401

402 Choi, U. S, Cho, Y. I and Kasza, K. E. 1992a. Degradation effects of dilute Polymer
403 Solutions on Turbulent Friction and Heat Transfer Behaviour. *Journal of Non-Newtonian
404 Fluid Mechanics*. 41, 289-307

405

406 Choi, U. S, France, D. M and Knodel, B. D. 1992b. Impact of advanced Fluids on Costs
407 of districts Cooling Systems. *Proceedings of 83rd Annual International Districts Heating
408 and Cooing Association Confrence*. Danves, Washington D C. 343-359.

409

410 Cogley, A. C, Vincent, W. G, Giles, S. E. 1968. Differential approximation to radiative
411 heat transfer in a non-grey gas near equilibrium, *The American Inst. Aeronautics and
412 Astronautics*.6:551-553.

413

414 Duncan, M. A and Rouvray, D. H, 1989. Microclusters. *Scientific American*, 110-115.

415

416 Feng, X, Ma, H and Huang S. 2006. Aqueous-organic phase-transfer of highly stable
417 gold, silver, and platinum nanoparticles and new route for fabrication of gold nanofilms
418 at the oil/water interface and on solid supports, *Journal of Physical Chemistry B*. 110(25)
419 12311–12317.

420

421 Gleiter, H, (1989). *Nanocrystalline Materials*. Programme on Materials Science. 33, 223-
422 315.

423 Hamilton, R. L and Crosser, O. K, 1962. Thermal Conductivity of Heterogeneous Two-
424 Component Systems. *Journal of Industrial and Engineering Chemistry Fundamentals*.
425 1(3), 187-191.

426

427 Hashin, Z and Shtrikman, S 1962. A variational Approach to the Theory of the Effective
428 Magnetic Permeability of Multiphase Materials. *Journal of Applied Physics*. 33(10),
429 3125-3131.

430

431 Hwang, Y, Lee, J. K. Lee, C. H . 2007. Stability and thermal conductivity characteristics
432 of nanofluids, *Thermochimica Acta*, 455(1-2),70–74.

433

434 Li, B. C .,1998. Nanotechnology in China. *Journal of Aerosol Science*. 29(5/6), 751-755.
435

436 Li, X. Zhu, D. and Wang, X. 2007. Evaluation on dispersion behavior of the aqueous
437 copper nanosuspensions, *Journal of Colloid and Interface Science*.310(2) 456–463.
438

439 Makinde, O. D and Mhone, P. Y. 2005. Heat Transfer to MHD Oscillatory Flow in a
440 Channel Filled with Porous Medium. *Romanian Journal of Physics*. 50, 931-938.
441

442 Mukherjee, S and Paria, S. 2013. Preparation and Stability of Nanofluids-A Review.
443 *IOSR Journal of Mechanical and Civil Engineering*. 9(2), 63-69
444

445 Nadeem, S and Saleem,S. 2004. Unsteady Mixed Convection Flow of Nanofluid on a
446 rotating cone with Magnetic Field. *Apply Nanoscience*. 4, 405-414.
447

448 Ngiangia, A.T and Harry, S T. 2017. Electroconductivity of Steady Viscous MHD
449 Incompressible Fluid Between Two Porous Parallel Plates Provoked by Chemical
450 Reaction and Radiation. *Physical Science International Journal* 13(2): 1-13.
451

452 Sebdani, S, Mahmoodi, M and Hashemi, S 2012. Effect of Nanofluid Variable Properties
453 on mixed Convection in a Square Cavity. *International Journal of Thermodynamic
454 Science*. 52, 112-126.
455

456 Sheikhzabeh, G. A, Hajialigol, N, Qomi, M. E and Fattahi, A. 2012. laminar Mixed
457 Convection of Cu-water Nanofluid in two sided lid-driven Enclosures. *Journal of
458 Nanostuctures*. 1, 44-53
459

460 Wasp. F., 1977. *Solid-Liquid Flow Slurry Pipeline Transportation*. Trans. Tech. Pub.,
461 Berlin.

462

463 Wei, X and Wang, L. 2010. Synthesis and thermal conductivity of microfluidic copper
464 nanofluids, *Particuology*. 8(3), 262– 271.

465

466 Xuan, Y and Li, Q., 2000. Heat transfer enhancement of nanofluids. *International Journal*
467 *of Heat and Fluid Flow* 21, 58-64.

468

469 Yu, W, Xie, H, Chen, L and Li, L. 2010. Enhancement of thermal conductivity of
470 kerosene-based Fe_3O_4 nanofluids prepared via phase- transfer method. *Colloids and*
471 *Surfaces A*. 355(1–3), 109–113.

472

473 Zhu, H. T. Zhang, C. Y. Tang, Y. M and Wang, J. X. 2007. Novel synthesis and thermal
474 conductivity of CuO nanofluid, *Journal of Physical Chemistry C*. 111(4) 1646–1650.

475

476

477

478

UNDER PEER REVIEW